Journal of Engineering Science and Technology
Vol. 18, No. 1 (2023) 310 - 330

AN INVESTIGATION ON THE SUPERIMPOSITION OF THERMAL DEGRADATION EFFECTS DUE TO SIMULTANEOUS FLOW MALDISTRIBUTION ON THE HOT AND COLD SIDES OF A CROSSFLOW HEAT EXCHANGER

W. M. CHIN

Daikin Research & Development Malaysia Sdn. Bhd., Jalan BRP 8/2, Taman Perindustrian Bukit Rahman Putra, 47000 Sg Buloh, Selangor, Malaysia
*E-mail: chinwm@daikin.com.my

Abstract

This paper reports the work done to investigate the hypothesis that the thermal degradation effect of a crossflow heat exchanger due to simultaneous flow maldistribution on the hot side and cold side fluid streams is a superimposition of the degradation effects due to the individual maldistributed flow acting by itself. The theoretical basis of the combined degradation is developed with a discretized heat exchanger model, where each discrete element is analysed as an individual cross-flow heat exchanger to derive a combined maldistribution thermal degradation factor, D_{combo}. A numerical calculation is then performed to verify the model, and comparison is made with other published data, and with experiments. The results from the study shows that D_{combo} can be approximated, in cases of maldistribution with low standard deviation and where $C_r = C_{min}/C_{max} \rightarrow 0$ with constant C_{max} fluid stream temperature, as the sum of the thermal degradation factors due to flow maldistribution acting individually in each flow passage. With larger standard deviations on the two fluid streams and with $C_r \rightarrow 1.0$, D_{combo} is less than the sum of the individual degradation factors. The findings from this work give useful insights on the interaction of the fluid streams leading to the combined thermal deterioration, and are useful to simplify the design process of crossflow heat exchangers within the established limits.

Keywords: Combined thermal degradation factor, Crossflow heat exchanger, Flow maldistribution, Superimposition of degradation effects.

1. Introduction

The thermal performance degradation of a heat exchanger due to flow maldistribution is well known. This has been a research topic discussed in many published literatures. Examples of these found in literature include the work done by Chiou [1, 2], Fagan [3], T'Joen et al. [4] and Koern et al. [5]. All of these works attempt to quantify the magnitude of thermal degradation as the degree of maldistribution changes. With this knowledge, the design of the heat exchanger can be changed, or corrected, to account for the loss of performance.

The thermal degradation factor D of a heat exchanger due to flow maldistribution has been correlated with the statistical moments of probability density function, i.e., mean, standard deviation and skew, which characterizes the flow maldistribution profile, for crossflow fin-tube heat exchangers [6, 7]. By far, the standard deviation is the most widely used parameter in the research on flow nonuniformity as a measure to quantify the dispersion of velocities from mean in a distribution. With the developed correlation equations obtained from [6, 7], the thermal performance of the heat exchanger can be predicted for any nonuniform air flow profile. In these works, the flow maldistribution occurs only on the air side of the exchanger, while the flow in the tube side is kept uniform. Other papers which have reported similar work on one-sided maldistribution include Beiler and Kroger [8], Elgowainy [9], Chin [10], Zhang et al [11] and Blecich et al. [12].

However, in any actual application, maldistribution inevitably occurs on all the fluid streams flowing through the heat exchanger. Literature review has shown many prior researches done on flow maldistribution on the hot and cold fluid streams in the exchanger. Examples of such work are the research done by Chiou [13] and Ranganayakulu et al. [14] on crossflow plate-fin heat exchangers. A similar work was also done by Yuan [15] for a 3-fluid crossflow heat exchanger. The results from these works have been presented in several series of graphs (thermal performance deterioration factor vs. NTU) depicting the degraded heat exchanger effectiveness with respect to the imposed non-uniform flow distribution in the flow channels.

More recent numerical and simulation works have also been done, e.g., Yang et al. [16] who performed CFD simulations on a parallel plate heat exchanger, under both counterflow and parallel flow configurations, to compare the effectiveness degradation rate of one-sided and two-sided flow maldistribution in the plate channels. Guo et al. [17] examined a crossflow heat exchanger with supercritical CO_2 as the fluid. Depending on the inlet flow maldistribution profiles in both channels and the coordination angle between heat transfer coefficient and temperature difference in the channels, both heat transfer deterioration and enhancement have been observed. They have suggested that the deterioration or enhancement effects of both hot and cold fluids could be superimposed together.

A numerical work was also conducted by Aasi and Mishra [18] on the dynamic response of a 3-pass cross flow heat exchanger undergoing different combination of flow maldistribution in the channels. With inlet temperature perturbations, the maldistributed flows in the three channels took longer time to reach steady state as compared to uniform flow. They have also observed heat transfer augmentation, of which the magnitude is dependent on the inlet flow maldistribution profiles.

There are also researches done where the flow maldistribution on one-side of the exchanger has induced a temperature maldistribution on the flow distribution

in the other side. Such studies are more related to the evaporators and condensers used in air-conditioning systems where the refrigerant or steam flowing in the tubes of fin-tube heat exchangers undergoes phase change. The flow maldistribution on the air-side induces unequal superheating or subcooling at the exit of the circuits in the exchanger.

Koern et al. [5, 19] have determined that significant recovery of the cooling capacity and COP degradation, due to maldistribution on both air-side and tube-side of the heat exchanger, can be achieved by controlling the superheat of individual circuits by re-distributing the mass flow rates. A similar conclusion was reached by Choi et al. [20] where 4% of capacity recovery was possible by controlling the exit superheat at 5.6^{o}C.

Lee and Domanski [21] have also observed that the performance deterioration is more sensitive to the air-side maldistribution than tube-side. Chng [22] has analysed the effect of non-uniform R32 refrigerant mass flow rate distribution in the tube circuits of a microchannel condenser coil while the air-side is uniform. A mathematical model of the thermal degradation factor was developed with the maldistribution statistical moments. It was highlighted that the magnitude of subcooling at the condenser outlet has significant effect on the thermal degradation, but not the inlet superheat.

All of these prior research works have demonstrated that the thermal performance degradation can be evaluated by means of numerical methods and simulations, or even by experimentation. However, such approaches may not be practical for design purposes due to the computational and testing costs. On the other hand, simple correlation equations have been proposed to calculate the thermal degradation factor due to one-side maldistribution [7, 22]. The literature review suggests that it could be possible to predict the magnitude of degradation for a given combination of non-uniform distributions in the exchanger hot and cold flow channels from the known results of each individual one-sided maldistribution, e.g. by superimposition, as pointed out by Guo et al. [17]. The exploration of such an approach has not been reported before in the literature.

Therefore, the work presented in this paper attempts to examine the hypothesis that the combined thermal degradation from simultaneous flow maldistribution on the hot and cold streams is equal to the sum of the thermal degradation effects caused by the individual maldistributions. The validity of this hypothesis will help to simplify the design of a heat exchanger. To do this, a mathematical model of the heat exchanger which is subjected to two flow maldistributions is firstly developed. A numerical calculation is then performed to verify the theoretical model where the statistical moments of both flow maldistributions are systematically changed to evaluate their influences on the thermal performance degradation. Lastly, a comparison is made with previous published data and with experimental data to validate the model.

2. Mathematical Model

Consider an arbitrary crossflow heat exchanger which has two fluid streams flowing through separate flow passages in it. A rectangular block of heat exchanger is modelled in this work as this shape of crossflow heat exchangers is commonly used in the industry, e.g. evaporator and condenser coils in air-conditioning and refrigeration equipment, steam and chilled water coils, air-to-air heat exchangers,

etc. Heat is transferred from the hot fluid, with inlet temperature T_h, through the walls of the passages, with surface temperature T_s, to the cold fluid side, with inlet temperature T_c, i.e., $T_h > T_s > T_c$. The transport of heat between the fluid and the walls is by means of convection, while conduction takes place through the wall thickness. This heat exchanger is shown in Fig. 1, which illustrates the crossflow configuration. The figure shows that the inlet face areas of the heat exchanger for the two fluids have been discretized into smaller cell elements. Both fluid streams also have non-uniform velocity profiles entering the heat exchanger inlets, i.e., $u_c(x, y)$ for the cold side and $u_h(y, z)$ for the hot side.

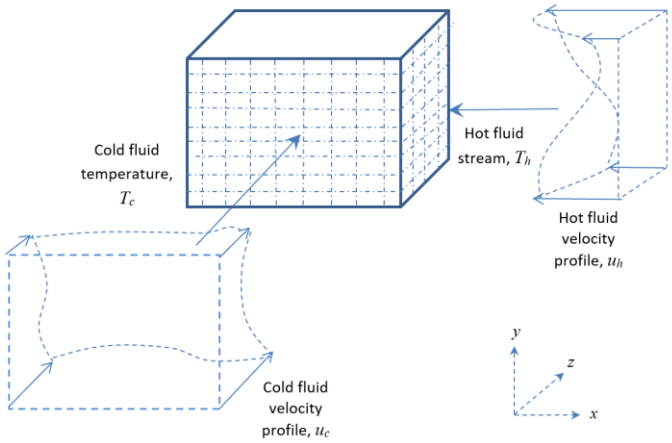

Fig. 1. Illustration of heat exchanger.

Each cell element in the heat exchanger is then identified with an index (i, j, k) in the x-, y- and z- directions respectively. In this model, the heat exchanger has a number of elements in the x-direction, b elements in the y-direction and c elements in the z-direction.

With the discretized grid on the heat exchanger, the non-uniform velocity profiles imposed on the two fluid inlets are also discretized. Therefore, each discrete cell element in the heat exchanger has a specific set of hot fluid and cold fluid velocities and it is treated as an individual cross-flow heat exchanger.

The following assumptions are used in this model:

- The inlet temperatures of the two fluid streams are constant and with uniform distribution.
- The convective heat transfer coefficient on the walls of the discreet cell passages is constant which is dependent on the fluid velocity flowing through the channel.
- The longitudinal heat transfer through the wall of successive discreet hot or cold cells is ignored.

The non-uniform velocity profiles on the heat exchanger are characterized by their statistical moments of probability density function, i.e., mean μ (1st moment), standard deviation σ (2nd moment), skew γ (3rd moment) and kurtosis κ (4th moment). It has been established by Chin and Raghavan [6, 7] that the thermal performance degradation arising from flow non-uniformity is significantly affected by the first three moments, but not by the kurtosis.

The thermal performance degradation of the heat exchanger as a result of flow maldistribution is determined by the degradation factor *D*, defined as [6]:

$$D = \frac{Q_u - Q_m}{Q_u} = 1 - \frac{Q_m}{Q_u} \quad (1)$$

For each discrete cell, the heat transfer rate q_{ijk} from the hot side to the cold side can be expressed as:

$$q_{ijk} = U_{o,ijk} A_{c,ijk} \Delta T_{h-c,ijk} \quad (2)$$

where $U_{o,ijk}$ is the overall heat transfer coefficient of the (*i*, *j*, *k*) element with reference to the inlet cold stream temperature, $A_{c,ijk}$ is the element's cold side heat transfer surface area and $\Delta T_{h\text{-}c,ijk} = T_{h,ijk} - T_{c,ijk}$ is the local mean temperature difference. Therefore, adding up all these discrete rates will give the total heat transfer capacity, *Q*, of the heat exchanger:

$$Q = \sum_{i=1}^{a} \sum_{j=1}^{b} \sum_{k=1}^{c} q_{ijk} \quad (3)$$

For the case of combined maldistributed flow in the two fluid streams, the total heat transfer capacity for the heat exchanger, which has total elements of $N = a$ x b x c, is given as:

$$Q_{m,combo} = \sum_N U_{o,ijk} A_{c,ijk} \Delta T_{h-c,ijk,m} \quad (4)$$

And the heat transfer capacity for the case of uniform flow on both the two fluid streams is given as:

$$Q_u = U_{o,u} \sum_N A_{c,ijk} \Delta T_{h-c,ijk,u} \quad (5)$$

where $U_{o,u}$ is the overall heat transfer coefficient of the heat exchanger with uniform flow distribution.

From Eqs. (1), (4) and (5), the thermal performance degradation factor due to the combined flow maldistribution on the two fluid streams can be expressed as:

$$D_{combo} = 1 - \frac{\sum_N U_{o,ijk} \Delta T_{h-c,ijk,m}}{U_{o,u} \sum_N \Delta T_{h-c,ijk,u}} \quad (6)$$

Next, consider the same heat exchanger which only has flow maldistribution on the cold side. The flow distribution on the other hot side is uniform. By using the same approach, the element heat transfer capacity is given as:

$$q_{ijk} = h_{c,ijk} A_{c,ijk} \Delta T_{s-c,ijk} \quad (7)$$

where h_c is the convective heat transfer coefficient on the cold surface and $\Delta T_{s\text{-}c} = T_s - T_c$ is the local temperature difference between the flow passage wall and the inlet cold fluid stream.

As a result, the thermal degradation factor due to flow maldistribution only on the cold fluid stream is derived as:

$$D_{cold} = 1 - \frac{\sum_N h_{c,ijk} \Delta T_{s-c,ijk,m}}{h_{c,u} \sum_N \Delta T_{s-c,ijk,u}} \quad (8)$$

Similarly, for the same heat exchanger which only has flow maldistribution on the hot side, while the other cold side has uniform flow distribution, the thermal degradation factor is given as:

$$D_{hot} = 1 - \frac{\sum_N h_{h,ijk,m} \Delta T_{h-s,ijk,m}}{h_{h,u} \sum_N \Delta T_{h-s,ijk,u}} \quad (9)$$

where $h_h$is the convective heat transfer coefficient on the hot surface of the heat exchanger and $\Delta T_{s\text{-}c} = T_h - T_s$ is the local temperature difference between the hot fluid stream and the heat exchanger wall.

Therefore, deducting Eqs. (8) and Eq. (9) from Eq. (6) gives the following expression:

$$D_{combo} - D_{cold} - D_{hot} = -1 - \left[\frac{\sum_N U_{o,ijk} \Delta T_{h-c,ijk,m}}{U_{o,u} \sum_N \Delta T_{h-c,ijk,u}} - \frac{\sum_N h_{c,ijk} \Delta T_{s-c,ijk,m}}{h_{c,u} \sum_N \Delta T_{s-c,ijk,u}} - \frac{\sum_N h_{h,ijk,m} \Delta T_{h-s,ijk,m}}{h_{h,u} \sum_N \Delta T_{h-s,ijk,u}}\right] \quad (10)$$

It is apparent that as the maldistributed flow becomes more uniform, i.e., as standard deviation $\sigma \rightarrow 0$, the corresponding maldistributed thermal resistance approaches that with uniform flow, which therefore causes the temperature differences to become the same. In other words, each of the three bracketed ratios in the R.H.S. of Eq. (10) approaches a magnitude of unity, and consequently making the R.H.S. to approach zero.

By equating the R.H.S. of Eq. (10) with the parameter δ, the equation is re-cast as:

$$D_{combo} = D_{hot} + D_{cold} + \delta \quad (11)$$

It can be seen from Eq. (11) that the parameter δ denotes the difference of the thermal degradation factor due to combined flow maldistribution with the addition of the thermal degradation factors due to the flow maldistribution acting by itself in the hot and cold fluid streams respectively. It is observed that the magnitude of δ is dependent on the relative magnitudes of the three bracketed ratios in Eq. (10). This is re-written as:

$$\delta = -1 - \frac{1}{N}\left[\sum_N U'_{o,ijk} \Delta T'_{h-c,ijk,m} - \sum_N h'_{c,ijk} \Delta T'_{s-c,ijk} - \sum_N h'_{h,ijk} \Delta T'_{h-s,ijk}\right] \quad (12)$$

The superscript ' for the heat transfer coefficients and temperature difference represent normalization with the corresponding values with uniform flow distribution. As mentioned, when $\sigma \rightarrow 0$, the three ratios on the R.H.S. of the equation approaches unity, i.e., $\delta \rightarrow 0$. Therefore, under the case of low maldistribution standard deviations, the combined thermal performance degradation factor can be estimated as the arithmetic sum of the individual degradation factors due to flow maldistribution of each fluid stream acting alone on the heat exchanger.

The magnitude of δ is also dependent on the relative magnitudes of the heat capacity ($C = \dot{m} c_p$) of the two fluid streams. In the case where one stream has a much higher C_{max} than the other C_{min}, i.e., $C_r = C_{min}/C_{max} \rightarrow 0$, the fluid temperature variations along the C_{max} flow direction are lesser; for example, a high flow rate of water and a flow of boiling or condensing fluid at saturation temperature. As a result, it can be deduced that either one of the second or third term in the bracketed R.H.S. of Eq. (12) would be close to 1, and $\delta < 0$. However, when both streams have comparable heat capacities, i.e., $C_r \rightarrow 1$, for example. in an air-to-air crossflow heat exchanger, the temperature variations within the channels of the heat exchanger would be larger. In such typical configurations where the heat transfer surface areas on the hot and cold fluid streams are equal, the heat transfer coefficients on both hot and cold streams would be about the same, i.e., $h_h \sim h_c =$

h, leading to the overall heat transfer coefficient, $U \sim h/2$. At the same time, the temperature difference between the hot and cold streams ($\Delta T_{h\text{-}c}$) would be approximately twice the temperature difference of the fluid with the channel wall surface ($\Delta T_{h\text{-}s} \sim \Delta T_{s\text{-}c}$). As a result, the bracketed term in the R.H.S. of Eq. (12) would become less than +1, and hence $\delta < 0$.

The following Table 1 summarizes the possible outcomes of δ from Eq. (12), where the bracketed terms are designated as A, B and C:

$$\delta = -1 - \frac{1}{N}\left[\sum_{N} U'_{o,ijk}\Delta T'_{h-c,ijk,m} - \sum_{N} h'_{c,ijk}\Delta T'_{s-c,ijk} - \sum_{N} h'_{h,ijk}\Delta T'_{h-s,ijk}\right] = -1 - [A - B - C] \quad (13)$$

Hence, it follows that δ would be less than or equal to zero.

As an extension, it is hypothesized that the derivation above can also be applied to a crossflow heat exchanger with any number of fluid streams (p) flowing through it. The general equation to describe the combined thermal degradation effect is then written as:

$$D_{combo} = \sum_P D_P + \delta \quad (14)$$

where P = 1, 2, 3, ... and $\delta \leq 0$.

Table 1. Summary of possible outcomes of δ.

Situation	δ	A	B	C
$\sigma \rightarrow 0$	$\rightarrow 0$	$\rightarrow 1$	$\rightarrow 1$	$\rightarrow 1$
$C_r \rightarrow 0$ C_{max} (on cold side) $T_c \sim$ constant ** $\Delta T_{s\text{-}c}$ approx. constant	$[C - A] < 0$ #		$\rightarrow 1$	
$C_r \rightarrow 0$ C_{max} (on hot side) $T_h \sim$ constant ** $\Delta T_{h\text{-}s}$ approx. constant	$[B - A] < 0$ @			$\rightarrow 1$
$C_r \rightarrow 1$	< 0	$-[A - B - C] < 1$		

Note #: $U'_{o,ijk}$ will be in the same order of magnitude as $h'_{h,ijk}$, and $\Delta T_{h\text{-}s} < \Delta T_{h\text{-}c.}$ Hence, [C – A] will be less than zero.
Note @: $U'_{o,ijk}$ will be in the same order of magnitude as $h'_{c,ijk}$, and, $\Delta T_{s\text{-}c} < \Delta T_{h\text{-}c.}$ Hence, [B – A] will be less than zero.
Note **: This situation corresponds to the fluid undergoing phase change without superheating or subcooling.

3. Numerical Simulation

A numerical simulation is performed on a crossflow fin-tube heat exchanger commonly used in air-conditioning and refrigeration equipment, to determine the thermal degradation effects due to the interaction of two maldistributed fluid streams. Hot water is used as the refrigerant flowing in the tubes while air flows in the channels created by the fins. Thus, the air-side of the heat exchanger is the cold stream while the water-side is the hot stream.

The numerical model is similar to that used in the previous work [7]. The specifications of the heat exchanger used in the simulation are listed in Table 2.

The air inlet face area is discretized into 100 elements while each of 10 tubes defines a discrete element on the water-side. In other words, a = 10, b = 10, c = 1, giving N = 100. This model is illustrated in Fig. 2 which also defines the inlet air and water temperatures. Each water inlet makes a single tube pass through the exchanger, while air passes through the fins on each discreet face area.

Table 2. Geometry of fin-tube heat exchanger.

Rows	1
Length	600 mm
Height	254 mm
Fin pitch	1.411 mm
Tube pitch	25.4 mm
Row pitch	22 mm
Tube diameter	9.52 mm
No. of tubes	10
Fin type	Wavy, corrugated
Corrugation angle	20°

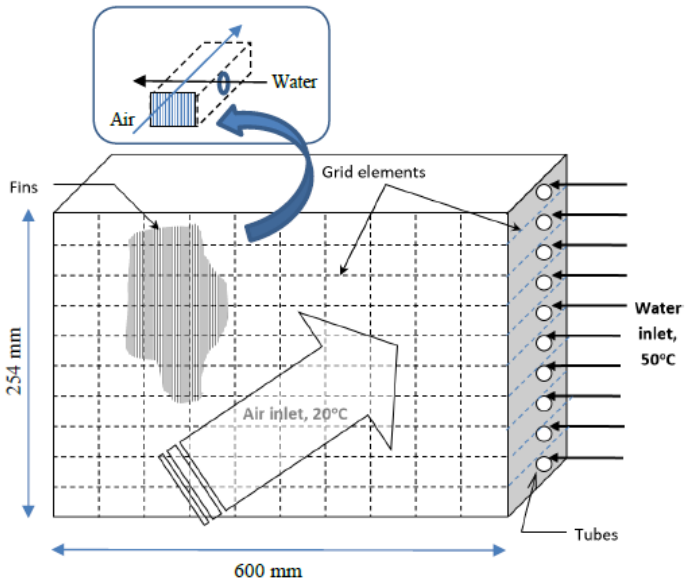

Fig. 2. Numerical model of fin-tube heat exchange. Inset: Zoom-in view of a discreet element showing the crossflow arrangement of air and water.

As a result of the discretization, each element of the heat exchanger has specific fluid velocities flowing through the fins and tubes. In the calculation, air passing through the fin passages is the fluid stream with minimum heat capacity rate, C_{min}.

The heat transfer coefficient on the air-side of the heat exchanger is calculated for each element at specific face velocities and fin geometry from known published correlation equations. In this work, the j-factor correlation developed by Wang et al. [23] for wavy fins is used, which is given as the following:

$$j = 0.324 Re_{Dc}^{J1} \left(\frac{F_p}{X_l}\right)^{J2} (tan\,\theta)^{J3} \left(\frac{X_l}{X_t}\right)^{J4} Nr^{0.428} \quad (15)$$

where

$$J1 = -0.229 + 0.115\left(\frac{F_p}{D_c}\right)^{0.6}\left(\frac{X_l}{D_h}\right)^{0.54} Nr^{-0.284}\, ln(\,0.5\, tan\,\theta) \quad (16)$$

$$J2 = -0.251 + \frac{0.232Nr^{1.37}}{(ln(Re_{Dc})-2.303)} \quad (17)$$

$$J3 = -0.439\left(\frac{F_p}{D_h}\right)^{0.09}\left(\frac{X_l}{X_t}\right)^{-1.75} Nr^{-0.93} \quad (18)$$

$$J4 = 0.502(ln(\,Re_{Dc}) - 2.54) \quad (19)$$

In the same manner, the heat transfer coefficient on the tube-side is calculated from the following equations:

For turbulent flow, Re_d > 10,000 (cited in [24]):

$$Nu = 0.023\,\mathrm{Re}_d^{\,0.8}\,\mathrm{Pr}^{\,0.4} \quad (20)$$

For transition flow, 2,300 < Re_d < 10,000 (cited in [25]):

$$Nu = \frac{(f/2)(Re_d - 100)Pr}{1+12.7(f/2)^{0.5}(Pr^{2/3}-1)} \quad (21)$$

where

$$f = \frac{1}{(1.58\,lnRe_d - 3.28)^2} \quad (22)$$

For laminar flow, Re_d < 2,300, and with constant tube wall temperature (cited in [25]):

$$\mathrm{Nu} = 3.66 \quad (23)$$

With these known, the overall heat transfer coefficient for each element is then calculated from the thermal resistance network equation, i.e., [24]:

$$\frac{1}{U_o A_c} = \frac{1}{\eta_{s,c} h_c A_c} + \frac{ln\left(D_o/D_i\right)}{2\pi k_w L A_c} + \frac{1}{\eta_{s,h} h_h A_h} \quad (24)$$

From this, the *NTU* of the element is calculated from the following relationship:

$$NTU = \frac{U_o A_c}{C_{min}} \quad (25)$$

The heat exchanger effectiveness is obtained from the known *ε-NTU* equation for a flow arrangement with both sides unmixed [24]:

$$\varepsilon = 1 - \exp\left[\left(\frac{1}{C_r}\right) NTU^{0.22}[\exp[-C_r NTU^{0.78}] - 1]\right] \quad (26)$$

The heating capacity of the heat exchanger element is then calculated from:

$$q_i = \varepsilon Cw, in_{a,in_{min}} \quad (27)$$

The temperature of air leaving each discrete element is obtained from the heating capacity, i.e.,

$$q_i = \dot{m}_a c_{pa}\left(T_{a,out} - T_{a,in}\right) \quad (28)$$

Similarly, the temperature of water leaving the element is calculated from:

$$q_i = \dot{m}_w c_{pw}\left(T_{w,in} - T_{w,out}\right) \quad (29)$$

For the discrete elements along each tube circuit, the leaving water temperature of a cell becomes the inlet temperature of the subsequent cell. Consequently, there

is a temperature differential between the water inlet and outlet of the heat exchanger. However, higher water flow rates result in smaller temperature differences which approximates the constant temperature assumption for the case of $C_r \rightarrow 0$ in the model.

With the numerical calculation procedure described above, the analysis is performed for the following cases:

(a) Uniform flow distributions on the air-side and tube-side
(b) Maldistributed flow on the air-side and uniform distribution on the tube-side
(c) Maldistributed flow on the tube-side and uniform distribution on the air-side
(d) Maldistributed flow on both the air-side and tube-side

For this purpose, 11 air-side and 9 tube-side discretized maldistribution profiles have been generated covering a range of standard deviation (between 0.10 and 0.60) and skew (between -1.00 and +1.00). It is noted that these maldistribution profiles have a normalized mean of 1.00. Following the findings from the previous work [6, 7], the effect of the kurtosis on the heat exchanger performance is not significant, and hence it is not examined in this work. These profiles are imposed onto the 10×10 air-side and 1×10 tube-side grids respectively.

In the calculation, the air flow rate varies between 0.20 and 1.00 m^3/s with an inlet temperature of 20 ^oC, while the hot water flow rate varies between 0.1 and 0.6 m^3hr^{-1} with inlet temperature of 50 ^oC. The fluid velocities for each discrete cell are therefore obtained by multiplying the respective normalized maldistribution profile with the average face velocity on both the fluid inlets.

The calculation procedure is performed by using Microsoft® EXCEL spread sheet with the aid of Visual Basic macro programming. The fluid velocities of the discretized elements of the heat exchanger are entered in rows, and Eqs. (15) to (29) are then applied in successive columns for each row to obtain the value of q_{ijk}. The air properties are taken from ASHRAE [26] where correlation equation for each property is developed with respect to the dry-bulb temperature. The refrigerant properties are obtained from the embedded REFPROP [27] functions in the spreadsheet. The summation of q_{ijk} is then compared with the corresponding case of uniform fluid distribution in both fluid streams to arrive at the thermal degradation factor.

4. Results and Discussion

The results of the numerical calculation are presented and discussed in the following sub-sections. Firstly, the results of the thermal degradation factors as the standard deviation of both fluid streams varies, while skew is held at zero, are shown in Fig. 3. Next, the effect of skew on the combined thermal degradation factor, D_{combo} is shown in Fig. 4. In Fig. 5, the effect of varying the flow rates, i.e., changing the mean fluid velocities, is presented.

4.1. Effect of standard deviation

The graphs shown in Fig. 3 illustrate the trend of D_{combo} as the standard deviation of the tube-side maldistribution, σ_{tube}, varies from 0.10 to 0.60 at three levels of air-side maldistribution standard deviation, σ_{air}. It is evident from the results that as the standard deviation of the two fluid streams increases, the thermal degradation increases.

It is also observed that the magnitude of D_{combo} is not very significant when the standard deviation is low, i.e., less than 2% when $\sigma < 0.20$. However, the thermal degradation effect becomes large when $\sigma > 0.60$, i.e., more than 20%.

More importantly, Fig. 3 shows that D_{combo} is approximately the same as the sum of thermal degradation factors, D_{air} and D_{tube}, acting alone in the heat exchanger, for values of standard deviation less than 0.40. A divergence of the trend lines is observed to occur when $\sigma > 0.50$ with D_{combo} becoming less than the sum $D_{air} + D_{tube}$. At $\sigma \sim 0.60$, the difference $\delta = -1.4\%$ (Fig. 3(c)).

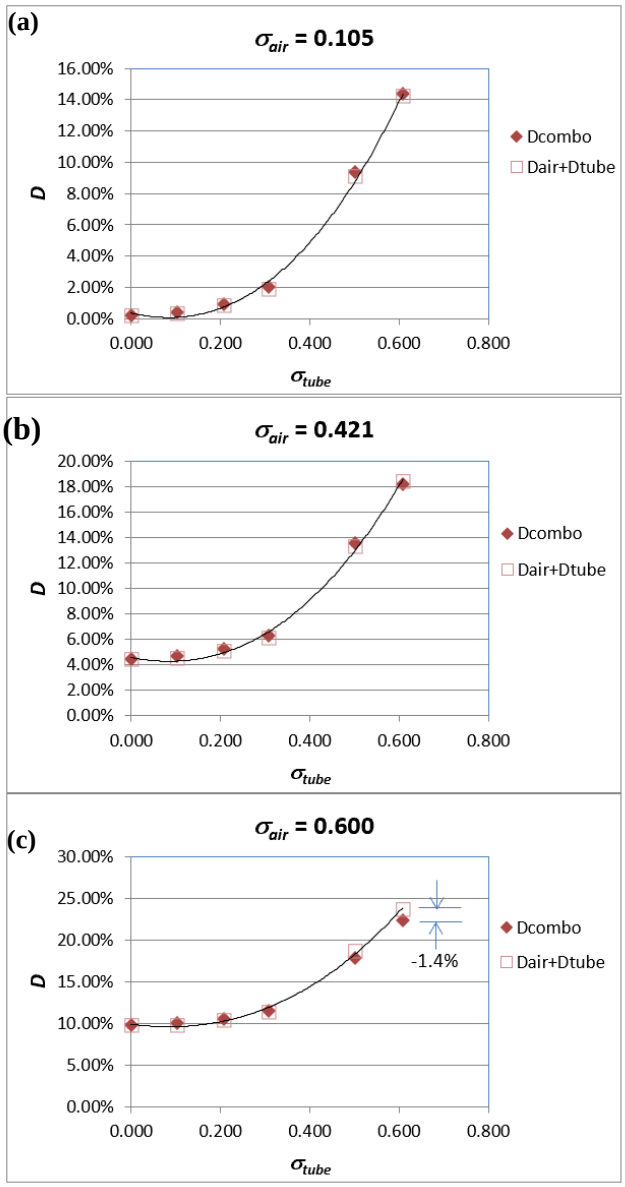

Fig. 3. Variation of *D* vs. standard deviation (Skew of both fluid sides = 0.00).

4.2. Effect of skew

The skews of both the air-side and tube-side maldistributions are kept the same at several magnitudes while the air-side standard deviation varies. In this numerical calculation, the tube-side standard deviation is also maintained (~ 0.46). The results of D_{combo} are plotted in Fig. 4 which shows the trend of D_{combo} vs. the magnitude of skew on both fluid sides. The difference δ is also calculated and plotted in Fig. 4.

The trend shown in Fig. 4 indicates that higher positive skews give lower magnitudes of thermal degradation. As expected, higher standard deviations shift the trend curve upwards, i.e., increasing D_{combo}, which is consistent with the results reported in the preceding section. It is also observed that the magnitudes of δ are negative.

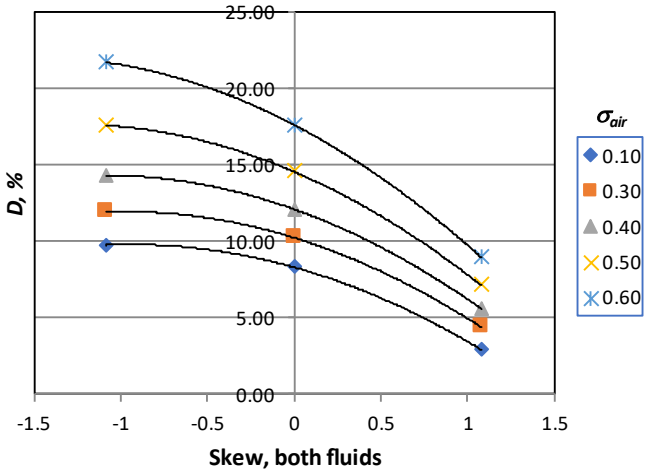

(a)

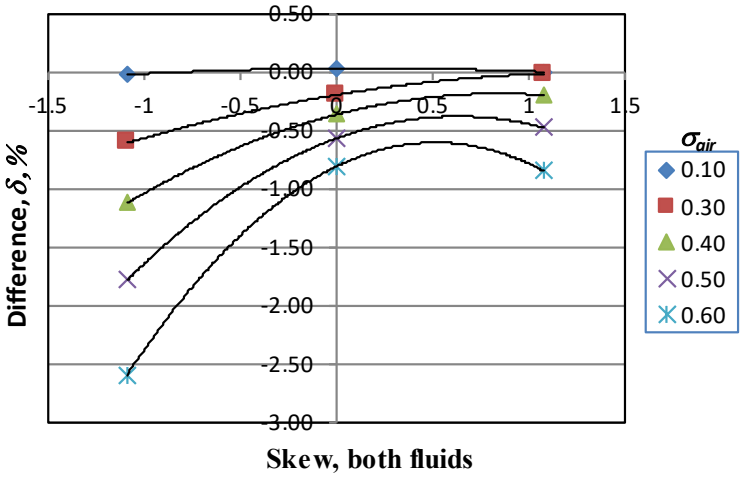

(b)

Fig. 4. (a) D_{combo}, % (b) Difference δ vs. with the same skew on both fluid sides (σ_{tube} ~ 0.46).

4.3. Effect of flow rate

It has been reported in the previous work [7] that the mean of the flow maldistribution can be represented with the non-dimensional parameter, *NTU*. Following Eq. (25), the total *NTU* for all the discretized elements of the heat exchanger is given as:

$$NTU = \frac{\sum_i U_{o,i} A_{o,i}}{\sum_i C_{min,i}} \tag{30}$$

As the air flow rate and mean air velocity increases, the magnitude of *NTU* decreases, and vice-versa.

The results from [7] have also demonstrated the significant dependence of *D* on the tube-side flow rates, which is represented by the internal heat transfer coefficient, h_w. Higher tube-side flow rates increase h_w which causes *D* to reduce. In this work, the effect of the tube-side flow rate is expressed with another non-dimensional parameter, N_i, which is defined as:

$$N_i = \frac{\sum_i h_{w,i} A_{w,i}}{\sum \dot{m}_w c_{pw}} \tag{31}$$

Higher tube-side flow rate lowers the value of N_i, and vice-versa.

With the range of air and water flow rates used in the numerical simulation, the magnitude of *NTU* varies between 0.25 and 0.80, while N_i varies between 0.33 and 0.42. For this simulation, the skew of the maldistribution on both the air and water sides are kept at zero. The results of the calculated D_{combo} as the *NTU* changes, for a fixed N_i, for different combination of standard deviations are shown in the following Fig. 5. The results of δ are also computed and plotted onto the same graph.

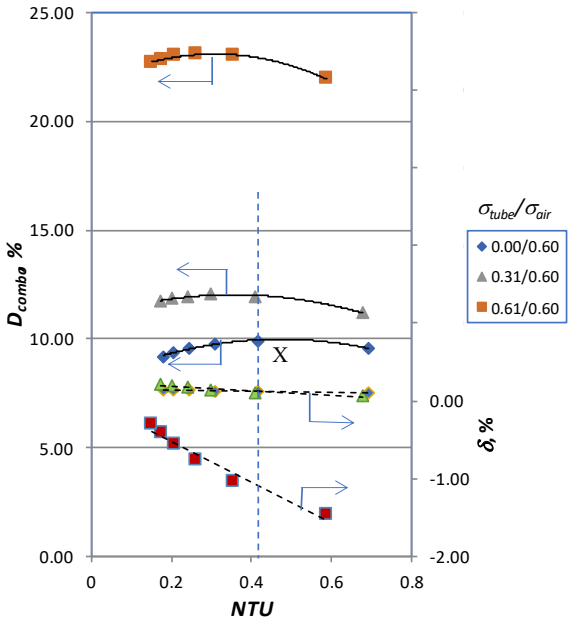

Fig. 5. Plot of D_{combo} and δ vs. *NTU* at specific air-side and tube-side standard deviations (N_i = 0.41, skew = 0.00).

The trend plot of Fig. 5 shows that when the tube-side distribution is uniform (i.e., σ_{tube} = 0.00), the thermal degradation factor for a specific air-side maldistribution has a maximum peak value. With σ_{air} = 0.60, this peak occurs at *NTU* = 0.42, as indicated by 'X'. The parabolic shape of this trend line is similar to that reported in [7]. As the tube-side maldistribution standard deviation increases, the peak shifts to the left towards lower *NTU* values.

Fig. 5 also illustrates the approximation of D_{combo} with D_{air} + D_{tube} where δ is approximately zero for σ_{tube} between 0.00 and 0.31. The negative magnitude of δ becomes more significant when the standard deviation of both fluid streams becomes larger. For example, at standard deviation of 0.60 for both air-side and tube-side, and *NTU* = 0.59, δ = -1.48%.

5. Comparison with Other Results

The developed derivation of the combined thermal degradation factor, i.e., Eq. (11), is compared with the results of the work done by Ranganayakulu et al. [14]. In that work, the thermal performance deterioration factor τ, for an air-to-air cross-flow heat exchanger was presented in a series of graphs. The definition of this factor is similar as D_{combo}. Plots of τ for the case of flow maldistribution occurring individually in each of the C_{min} and C_{max} streams are given, which is then accompanied with the plot where both the flow maldistributions act together.

For this comparison, data for heat capacity ratio, C_r = 1.0 with standard deviation of 0.11, 0.54 and 0.97 is used. The data points cover a range of *NTU* between 2 and 20. The values of τ obtained from the individually acting maldistributions are then added arithmetically (τ_{sum}) and compared with that from the combined maldistributions of both streams (τ_{combo}). The results of this comparison are shown in the following Fig. 6.

It is clear from the plots in Fig. 6 that the thermal degradation factor with combined non-uniform distribution in both fluid streams is lesser than the arithmetic sum of degradation factors for each flow maldistribution action alone, i.e., $\delta < 0$. In this work, the difference δ is significantly larger at higher standard deviations. With σ = 0.97, δ is up to -30%. Unlike the water-to-air fin-tube heat exchanger examined in the numerical model, the thermal resistances on both the hot and cold sides of the cross-flow heat exchanger are of the same order of magnitude (C_r = 1.0). As pointed out earlier, this would give rise to larger variations of local temperature differences between the fluid streams within the flow channels of the exchanger, causing larger magnitudes of δ.

Next, the results reported by Chowdhury and Sarangi [28] are examined. In this work, the multipassage heat exchanger ineffectiveness was calculated for two cases, i.e., One-side Nonuniformity (OSN) and Both-sides Nonuniformity (BSN). The ineffectiveness has the same meaning as the thermal degradation factor used in this paper. In both cases, the maldistributed profiles flowing in the nonuniform passages were generated by using a beta distribution function, B(p, q,). For the same parameters p = 1.1 and q = 1.1, the ineffectiveness of OSN and BSN are plotted vs. the distribution relative spread (which is analogous to standard deviation). The following Fig. 7 is a plot of the data extracted from the original paper.

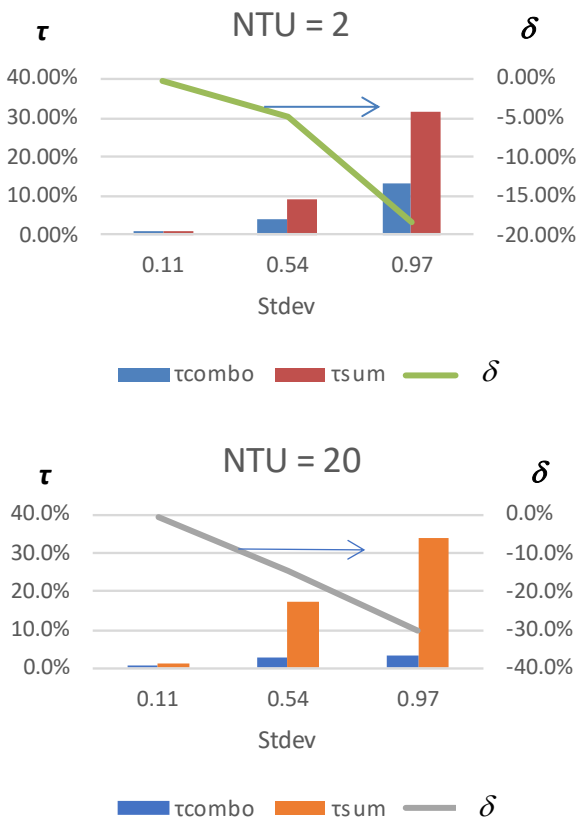

Fig. 6. Comparison of τ between combined non-uniformity on both sides with the arithmetic sum of individual sides (C_r = 1.0) [14].

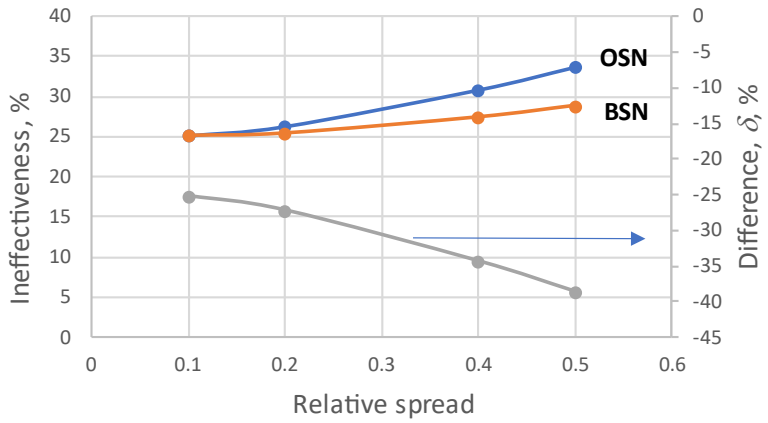

Fig. 7. Results of heat exchanger ineffectiveness with OSN and BSN nonuniform flow profile generated with B(1.1, 1.1) for NTU = 3.0 and C_r = 1.0 . Data is read from the original graph published in [28].

The difference, δ, is calculated by considering the same ineffectiveness of OSN for either side of the heat exchanger. This is also shown in Fig. 7 which clearly show the negative values of δ.

A similar comparison is then made with the results presented by Yang et al. [16] for a parallel plate-fin heat exchanger with counter-flow arrangement. The results reported, with a nonuniform velocity profile Configuration A acting on one-side and both-sides of the exchanger, are given in Fig. 8. The thermal degradation due to the maldistribution was quantified by using an effectiveness degradation rate, $\Delta\varepsilon$. The findings indicate that the degradation rate is lower when the same maldistribution flows on both sides of the passages as compared with one-sided maldistribution. Consequently, by considering the same degradation rate for either side of the exchanger, it can be calculated that the difference, δ, would also be negative.

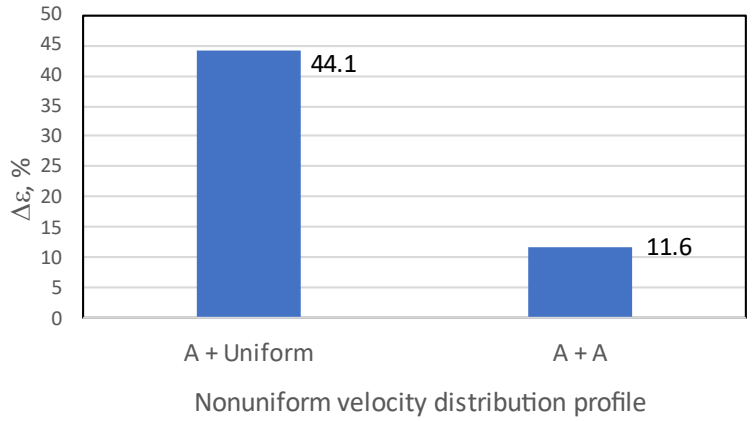

Fig. 8. Results of effectiveness degradation rate for (a) Configuration A and Uniform, (b) two-sided Configuration A, (A + A). Flow in counter-flow arrangement with Re = 100,000 to 600,000. [16].

An experiment is also carried out to validate the situation with $C_r \rightarrow 0$, i.e., by passing two-phase evaporating refrigerant (R-410A) through the tubes of the heat exchanger, while air passes through the fin passages. The test rig used for this experiment is shown in Fig. 9.

In this experiment, the air dry-bulb (DB) and wet-bulb (WB) temperatures entering the test coil is maintained at (27.0 ± 0.2) °C and (19.0 ± 0.2) °C respectively, with a flow rate of 0.33 m^3/hr (~ 715 ft^3/min). The R-410A refrigerant flow rate is also maintained at 43 kg/hr with an entering saturated temperature of (16.0 ± 0.5) °C. The air-side maldistribution profile is varied by covering certain portions of the coil face area with pieces of paper, while the refrigerant-side maldistribution is changed by adjusting the three throttling valves for the three separate serpentine circuits in the coil.

The test is initially run under uniform air and refrigerant distribution. Then, the air-side maldistribution is imposed on the coil while the refrigerant is kept uniform. This is then repeated by imposing refrigerant maldistribution while the air is uniformly distributed. Next, several combinations of air and refrigerant maldistributions are imposed simultaneously. In each case, the entering and leaving

air DB/WB are recorded, and the cooling capacity of the evaporator is calculated. From these, the maldistribution thermal degradation factor is computed.

The results of this experiment are summarized in Fig. 10.

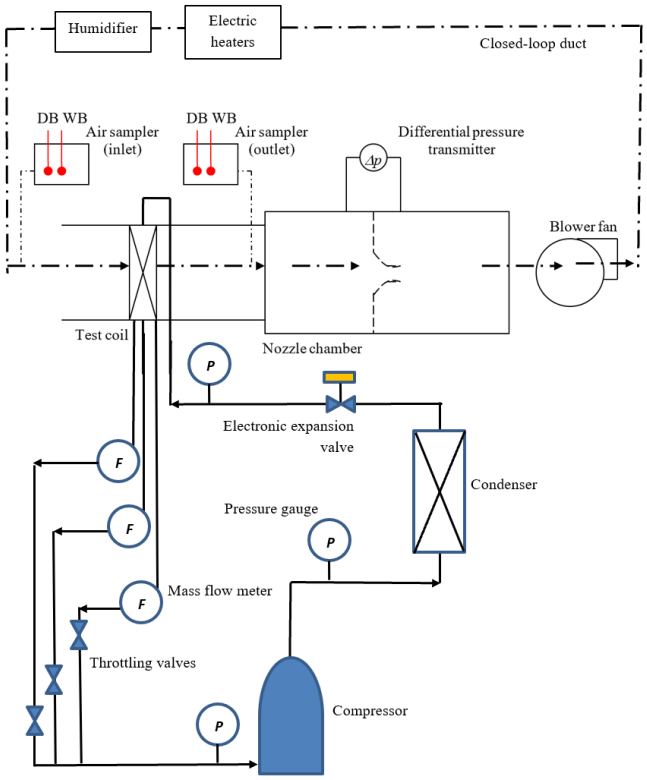

Fig. 9. Schematic diagram of test rig (simplified).

	Stdev	Dindividual
Air-side 1	0.637	4.50%
Air-side 2	0.754	5.72%
Air-side 3	0.911	6.01%
Tube-side 1	0.104	4.72%
Tube-side 2	0.143	6.38%

Combination		Dcombo	Dsum
Air-side 2 Tube-side 2	1	10.70%	12.10%
Air-side 3 Tube-side 1	2	10.12%	10.74%
Air-side 1 Tube-side 2	3	10.16%	10.88%
Air-side 2 Tube-side 1	4	9.84%	10.44%

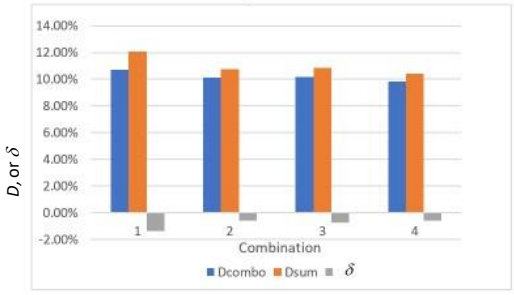

Fig. 10. Results of combined maldistribution experiment.

The experiment results clearly show that $\delta < 0$. However, the magnitude of δ is much smaller, i.e., between 0% to 2%. This concurs with the aforementioned analysis for the case of $C_r \rightarrow 0$ where it is seen that the combined thermal degradation factor is approximately the same as the sum of the individual degradation factors. Nevertheless, the observed negative magnitude of δ could also be due to the change of refrigerant vapour quality in the tubes, as pointed out in [10].

6. Conclusion

In conclusion, the results from this work have indicated that the superimposition hypothesis of the thermal degradation factors, i.e., that the combined thermal degradation factor from simultaneous flow maldistribution on the hot and cold streams is equal to the sum of the thermal degradation effects caused by the maldistribution acting alone in the respective flow passages, is applicable for a crossflow heat exchanger under certain conditions. These conditions include flow maldistributions with low standard deviation, $\sigma \rightarrow 0$, and when the C_{max} of one of the fluid streams is much larger than C_{min} ($C_r \rightarrow 0$), and where the temperature of the C_{max} fluid stream is constant. As the flow maldistribution standard deviation σ becomes larger, and when $C_r \rightarrow 1.0$, the deviation from the hypothesis increases. It is found that the combined degradation factor, D_{combo}. is lesser than, or equal to, the arithmetic sum of individual degradation factors, i.e., $\delta \leq 0$. Hence, the hypothesis can help to simplify the design process of crossflow heat exchangers from prior knowledge of individual maldistribution degradation effects, but within the applicability limits determined.

Nomenclatures

A	Area, m^2
C	Constant
C_{min}	Minimum heat capacity rate, W/K
C_{max}	Maximum heat capacity rate, W/K
C_r	Ratio of minimum to maximum heat capacity rate (=C_{min}/C_{max}), -
c_p	Specific heat at constant pressure, J/kg.K
D	Thermal performance deterioration factor, -
D_c	Fin collar diameter, m
D_h	Hydraulic diameter, m
D_i	Internal tube diameter, m
D_o	Outer tube diameter, m
f	Friction factor, -
F_p	Fin pitch, m
h	Heat transfer coefficient, $W/m^2.K$
i	Index
j	Colburn j-factor, or index
k	Thermal conductivity, W/m.K, or index
L	Tube length, m
$\dot{m}$	Mass flow rate, kg/s
N	Number of elements
N_i	Non-dimensional parameter defined in Eq. (30)
Nr	Number of tube rows

NTU	Number of transfer units, -
Nu	Nusselt number, -
n	Exponent
Pr	Prandtl number
Q, q	Heat transfer capacity, kW
R	Thermal resistance, K/W
Re	Reynolds number, -
T	Temperature, ^{o}C
U_o	Overall heat transfer coefficient, W/m^2.K
u	Velocity, m/s
x, y, z	Coordinate

Greek Symbols

μ	Mean
σ	Standard deviation
γ	Skew
κ	Kurtosis
δ	Difference of thermal degradation factor
ΔT	Temperature difference, ^{o}C
θ	Fin corrugation angle, ^{o}
η_s	Fin surface efficiency, %
ε	Heat exchanger effectiveness, %
τ	Thermal performance deterioration factor, -

Symbols

~	Approximately

Subscripts

a	Air
combo	Combined
cold, c	Cold stream
d	Tube diameter
Dc	Fin collar diameter
hot, h	Hot stream
i	Element number
m	Maldistributed
s	Surface
u	Uniform
w	Wall, or water

Superscripts

‘	Normalized

References

1. Chiou, J.P. (1978). Thermal performance deterioration in crossflow heat exchanger due to the flow nonuniformity. *ASME Journal of Heat Transfer*, 100(4), 580-587.

2. Chiou, J.P. (1985). The effect of the air flow nonuniformity on the thermal performance of automobile air conditioning condenser. *SAE Technical Paper* 830542.
3. Fagan, T.J. (1980). The effects of air flow mal-distributions on air-to-refrigerant heat exchanger performance. *ASHRAE Transactions*, 86(2), 699-713.
4. T'Joen, C.; Willockx, A.; Steeman, H.-J.; and De Paepe, M. (2007). Performance prediction of compact fin-and-tube heat exchangers in maldistributed airflow. *Heat Transfer Engineering*, 28(12), 986-996.
5. Kærn, M.R.; Brix, W.; Elmegaard, B.; and Larsen, L.F.S. (2011). Compensation of flow maldistribution in fin-and-tube evaporators for residential air-conditioning. *International Journal of Refrigeration*, 34(5), 1230-1237.
6. Chin, W.M.; and Raghavan, V.R. (2011). On the adverse influence of higher statistical moments of flow maldistribution on the performance of a heat exchanger. *International Journal of Thermal Sciences*, 50(4), 581-591.
7. Chin, W.M.; and Raghavan, V.R. (2011). The influence of the moments of probability density function for flow maldistribution on the thermal performance of a fin-tube heat exchanger. *International Journal of Thermal Sciences*, 50(10), 1942-1953.
8. Beiler, M.G.; and Kroger, D.G. (1996). Thermal performance reduction in air-cooled heat exchangers due to nonuniform flow and temperature distributions. *Heat Transfer Engineering*, 17(1), 82-92.
9. Elgowainy, A. (2003). Effect of airflow mal-distribution on pressure drop and thermal performance of heat exchangers in residential heat pump systems. *ASHRAE Transactions*, 109(2), 9-14.
10. Chin, W.M. (2017). On the phenomenon of two-phase flow maldistribution in a heat exchanger undergoing condensation. *Journal of Engineering Science and Technology* (*JESTEC*), 12(8), 2028-2045.
11. Zhang, K.; Li, M.-J.; Liu, H.; Xiong, J.-G.; and He, Y.L. (2021). A general and rapid method to evaluate the effect of flow maldistribution on the performance of heat exchangers. *International Journal of Thermal Sciences*, 170, 107152.
12. Blecich, P.; Trp, A.; and Lenić, K. (2021). Thermal performance analysis of fin-tube heat exchangers operating with airflow nonuniformity. *International Journal of Thermal Sciences*, 164, 106887.
13. Chiou, J.P. (1978). Thermal performance deterioration in a crossflow heat exchanger due to the flow nonuniformity on both hot and cold sides. *Proceedings of the 6th International Heat Transfer Conference*, Toronto, Canada, 4, 279-284.
14. Ranganayakulu, C.H.; Seetharamu, K.N.; and Sreevatsan, K.V. (1997). The effects of inlet fluid flow non-uniformity on thermal performance and pressure drops in cross-flow plate-fin compact heat exchangers. *International Journal of Heat and Mass Transfer*, 40(1), 27-38.
15. Yuan, P. (2003). Effect of inlet flow maldistribution on the thermal performance of a three-fluid crossflow heat exchanger. *International Journal of Heat and Mass Transfer*, 46(20), 3777-3787.

16. Yang, H.; Wen, J.; Gu, X.; Liu, Y.; Wang, S.; Cai, W.; and Li, Y. (2017). A mathematical model for flow maldistribution study in a parallel plate-fin heat exchanger. *Applied Thermal Engineering*, 121, 462-472.
17. Guo, J.; Huai, X.; Cheng, K.; Cui, X.; and Zhang, H. (2018). The effects of nonuniform inlet fluid conditions on crossflow heat exchanger. *Internal Journal of Heat and Mass Transfer*, 120, 807-817.
18. Aasi, H.K.; and Mishra, M. (2020). Influence of flow non-uniformity on the dynamic behaviour of three-fluid cross-flow compact heat exchanger. *International Journal of Thermal Sciences*, 149, 106177.
19. Kærn, M.R.; Brix, W.; Elmegaard, B.; and Larsen, L.F.S. (2011). Performance of residential air-conditioning systems with flow maldistribution in fin-and-tube evaporators. *International Journal of Refrigeration*, 34(3), 696-706.
20. Choi, J.M.; Payne, W.V.; and Domanski, P.A. (2003). Effects of non-uniform refrigerant and air flow distributions on finned-tube evaporator performance. *Proceedings of the 21st International Congress of Refrigeration*, Article no. ICR0040, Washington, D.C., 1-8.
21. Lee, J.; and Domanski, P.A. (1997). Impact of air and refrigerant maldistributions on the performance of finned-tube evaporators with R-22 and R-407C. *Final Report*, ARTI MCLR Project Number 665-54500.
22. Chng, M.H. (2016). *Development of Refrigerant* (*R*32) *Flow maldistribution model for microchannel heat exchanger*. Doctoral Thesis, Universiti Putra Malaysia.
23. Wang, C.-C.; Jang, J.-Y.; and Chiou, N.-F. (1999). Technical note: A heat transfer and friction correlation for wavy fin-and-tube heat exchangers. *International Journal of Heat and Mass Transfer*, 42(10), 1919-1924.
24. Incropera, F.P.; and DeWitt, D.P. (2002). *An introduction to heat transfer* (4th Ed.), New York: Wiley.
25. Rohsenow, W.H.; Hartnett, J.P.; and Cho, Y.I. (1998). F*orced convection, internal flow in ducts, handbook of heat transfer* (3rd Ed.), New York: McGraw Hill.
26. ASHRAE Handbook, Fundamentals (2009). Psychrometrics.
27. NIST Reference Fluid Thermodynamic and Transport Properties Database (REFPROP), Version 9 (2010).
28. Chowdhury K.; and Sarangi S. (1985). Effect of flow maldistribution on multipassage heat exchanger performance. *Heat Transfer Engineering*, 6(4), 45-54.